HIGH HARMONIC SOURCE FOR SEEDING OF FERMI@Elettra

S.J. Goh[a*], P.J.M. van der Slot[a], H.J.M. Bastiaens[a], S.G. Biedron[b,c], M.B. Danailov[b],
S.V. Milton[b,c], J. Herek[d], K.J. Boller[a]
[a] Laser Physics and Nonlinear Optics, [d] Optical Sciences,
Mesa+ Institute for Nanotechnology, University of Twente, Enschede, The Netherlands
[b] FERMI@Elettra, Sincrotrone Trieste S.C.p.A., Basovizza, Trieste, Italy
[c] Argonne National Laboratory, Argonne, Illinois, USA

Abstract

FERMI@Elettra is a free electron laser user facility that will produce high-brightness, ultra-short pulses with broad wavelength coverage for a wide range of user experiments. Currently, FERMI uses the HGHG technique to improve both the longitudinal and spectral coherence and the stability of the output of the laser. Using a High Harmonic (HH) source to drive the HGHG process will allow FERMI to reach shorter wavelengths with a single stage. It also will provide a comparison between HH and HGHG seeding methods. For the HH source, we will use neutral atoms in a hollow waveguide in combination with pulse shaping of the drive laser pulse to provide wavelength tuning as well as selective enhancement of the harmonic orders. In this paper, we the discuss the scaling of HH generation to several hundreds of nanoJoule pulse energy at a specific harmonic (several tens of MW peak power) and present the HH source under construction at the university of Twente.

INTRODUCTION

FERMI@Elettra is a free electron laser (FEL) user facility currently under commissioning at Sincrotrone Trieste S.C.p.A. Its goals are to produce high-brightness, ultra-short pulses with wavelengths ranging from 100 - 20 nm (FEL1) and 40 - 4 nm (FEL2) and deliver these pulses to a wide range of user experiments. Currently, FERMI uses the high gain harmonic generation (HGHG) technique to improve both the stability and the longitudinal and spectral coherence of the output of the laser. FEL1 uses a single stage downshift, while FEL2 will use cascaded HGHG to reach a fundamental wavelength as short as 4 nm. The seed laser wavelength for both the single stage and the double stage HGHG is between 195 nm and 280 nm.

Replacing the drive laser for the single stage HGHG by a high harmonic (HH) source will extend the final wavelength of the single stage HGHG towards much shorter wavelengths. Also, direct seeding of FEL1 using the HH-source is possible and will allow a direct comparison between the two seeding methods. Initially HH seeding will be done in the wavelength range of 60 to 30 nm, corresponding to harmonics 13 to 27 for a drive laser wavelength of 800 nm. Various noble gasses have been used as a source for EUV light [1, 2] and the particular choice depends on balancing gain and absorption losses at the desired order for a particular noble gass. For example, Ar shows a higher absorption than Xe at the longer wavelengths within the range of interest and therefore Xe will be used for wavelengths close to 60 nm and Ar for wavelengths close to 30 nm [3]. In the remaining part of this paper we will only consider Argon as this medium covers the shorter part of the wavelength range and has consequently a lower conversion efficiency.

The HH source is based on harmonic generation from neutral atoms in a hollow waveguide (capillary) in combination with coherent control of the drive laser pulse to provide wavelength tuning as well as selective enhancement of a specific harmonic. Pressure tuning will be used to obtain phase matched high order harmonic generation [4, 5]. The process of generating high harmonics by an intense, linear polarised drive laser pulse can be described by the so-called three step model [6]. First the high electric field of the drive laser pulse induces tunnel ionisation, then the electron is driven away from the ion by the same electric field. When the field reverses direction the electron is driven back to the ion and can recombine. At recombination, the sum of the kinetic energy of the electron and ionisation energy is emitted as a short burst of short wavelength radiation.

Using 20 fs pulses from a Ti:Sapphire laser it was shown that orders 23 to 31 (34.9 - 25.8 nm) could be phase matched in a 150 μm diameter capillary with a length of 30 mm and filled with Ar by varying the pressure from 40 to 66 mbar [4]. Using an input energy of 100 to 300 μJ a conversion efficiency of 10^{-6} to 10^{-5} was reported [4]. A seed power of $\sim 1\,\mathrm{MW}$ is required to generate the 5^{th}, and maybe the 6^{th} harmonic using the single stage HGHG section of FEL1, Therefore, the drive laser energy for high harmonic generation (HHG) needs to be increased by at least an order of magnitude. We investigate how we need to scale HHG when we increase the drive laser pulse energy from 0.2 mJ to 6 mJ. In the remaining part of this paper we discuss this scaling and describe the proposed HH source. We conclude with the expected improvement of conversion efficiency.

SCALING OF HHG

Efficient generation of high harmonics requires phase matching between the drive laser and the generated harmonics (see e.g., [1, 4]). We consider here the case of high harmonic generation from neutral atoms inside a hollow

---

[*] s.j.goh@utwente.nl

capillary. The magnitude of the wave vector, k of a wave propagating through the capillary is given by

$$k \approx \frac{2\pi}{\lambda} + \frac{2\pi N_a \delta(\lambda)}{\lambda} - N_e r_e \lambda - \frac{u_{11}^2 \lambda}{4\pi a^2}, \quad (1)$$

where λ is the free space wavelength, N_a is the neutral atom density in the capillary, δ is the real part of $n-1$ per atom, n is the index of refraction, N_e is the electron density that results from ionisation, r_e is the classical electron radius, u_{11} is the first root of the Bessel function of the first kind J_0, and a is the inner radius of the capillary. Both N_a and N_e are proportional to the pressure, and, when we assume that the neutral atoms are only singly ionised, N_a is proportional to $P(1-\eta)$ and N_e with $(P\eta)$, where P is the pressure and η is the ionisation fraction.

From eq. 1, the phase mismatch $\Delta k = k_q - qk_f$ can be calculated, where $k_f = \frac{2\pi}{\lambda_f}$ is the wave vector of the fundamental, q is the harmonic number and $k_q = \frac{2\pi}{\lambda_q}$ the wave vector of the harmonic, as

$$\Delta k = -\frac{2\pi}{\lambda_q} N_a \Delta_q + N_e r_e (q\lambda_f - \lambda_q) + \frac{q\lambda_f - \lambda_q}{4\pi} \frac{u_{11}^2}{a^2}. \quad (2)$$

Here $\Delta k = \delta(\lambda_f) - \delta(\lambda_q)$ is the difference in real part of the index of refraction at the fundamental and harmonic wavelength. Eq. 2 expresses that the phase mismatch contains three contributions. The first is due to dispersion of the neutral atoms, the second is due to the dispersion of the free electron density and the last is due to dispersion of the hollow capillary. For simplicity we ignore the intensity dependent phase lag due to the difference in moment of ionisation and recombination. This phase lag is approximately independent of the driving electric field for the so-called short electron trajectories, and electrons following these trajectories are dominantly responsible for the harmonics observed when a capillary is used [7].

Eq. 2 shows under what conditions phase matching ($\Delta k = 0$) can be obtained in a capillary. When the intense drive laser pulse propagates through the capillary, it will ionise the gas. As a result, the neutral fraction decreases and the free electron density grows at the same time. Hence, at a given pressure the net dispersion due the neutral atoms and free electrons changes and can just compensate the dispersion due to the geometry at a certain ionisation level. As the drive laser intensity varies both in time and with radial position, the ionisation fraction, and thus the phase matching, shows a strong temporal and spatial dependency. The phase mismatch Δk determines a coherence length $L_{coh} = \frac{\pi}{\Delta k}$, which defines the spatial region over which the emission of a particular harmonic shows constructive interference.

To determine the ionisation fraction, we use the ionisation rate $w(t)$ in the strong-field limit (Ammosov, Delone, and Krainov (ADK) model) [8],

$$w(t) = \omega_p |C_{n^*}|^2 \left(\frac{4\omega_p}{\omega_t}\right)^{2n^*-1} e^{-\frac{4\omega_p}{3\omega_t}} \quad (3)$$

with

$$\begin{aligned} \omega_p &= \frac{I_p}{\hbar} \\ \omega_t &= \frac{eE_d(t)}{(2mI_p)^{\frac{1}{2}}} \\ n^* &= Z\left(\frac{I_p}{I_h}\right)^{\frac{1}{2}} \\ |C_{n^*}|^2 &= 2^{2n^*}[n^*\Gamma(n^*+1)\Gamma(n^*)]^{-1}. \end{aligned}$$

Here, I_p is the ionisation potential of the atom, I_h is the ionisation potential of the hydrogen atom, e is the electron charge, m is the electron mass, and E_d is the modulus of the instantaneous electric field of the drive laser pulse. Eq. 3 assumes ionisation from the ground state of the atom. From the ionisation rate, $w(t)$, the fraction of free electrons $\eta(t) = N_e/N_0$, with N_0 the initial atom density, can be calculated from a rate equation, yielding

$$\eta(t) = 1 - exp(-\int_{-\infty}^{t} w(t')dt'). \quad (4)$$

Note that $1 - \eta(t)$ is equal to the ionisation probability.

To calculate the absolute intensity generated at a particular harmonic requires a complicated model that calculates the atomic response A_q at the desired harmonic q. However, for a scaling study, it is sufficient to calculate the intensity build-up based on both phase matching and absorption in the generating medium. This build-up can be modeled by [9]

$$N_q \propto N_a^2 A_q^2 \frac{1 + e^{-2\alpha L_m} - 2\cos(\Delta k L_m) e^{-\alpha L_m}}{\alpha^2 + \Delta k^2}, \quad (5)$$

where L_m is the length of the capillary (medium), $\alpha = \frac{1}{2L_{abs}}$, and L_{abs} is the intensity absorbtion length at the harmonic wavelength. To include the ground state depletion as well as the intensity dependence of the harmonic response we set $A_q \propto (1-\eta)|E_d|^5$ [1, 9]. To calculate the relative output, we first use eq. 3 to calculate the local ionisation fraction as a function of the position of time in the drive laser pulse and radial postion in the cross-section of the capillary. Then this ionisation factor is used to calculate the local phase mismatch using eq. 2. Finally, eq. 5 is used to calculate for each radial position and each time in the drive laser pulse the contribution to the output at harmonic q. By integrating over the pulse and cross-section of the capillary, we obtain the total relative output. Note, the largest contribution to this output is coming from the region where the generation is phase matched, i.e., where $\Delta k = 0$. The drive laser field strength in this region is such that the conditions for eq. 3 apply. However, they fail near the wall of the capillary and at the front and back side of the laser pulse. This will not affect the output calculation as (i) the ionisation level will be to low for phase matching (i.e., large $|\Delta k|$ and (ii) the local field amplitude is to low to generate the desired harmonic.

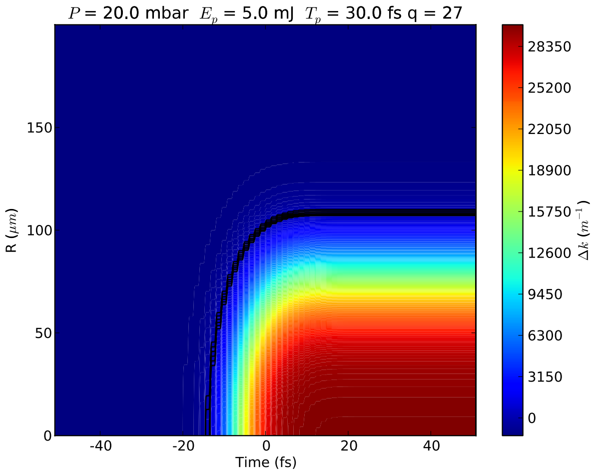

Figure 1: Phase mismatch Δk as a function of radial position and time in the drive laser pulse. The black line indicates where phase matching occurs $(\Delta k = 0)$

To verify the validity of this model, we compare the calculated performance with measurements performed by Rundquist et al. [4]. They measured the output of the 29^{th} and 31^{st} harmonic as a function of pressure. Our model predicts maximum output for each harmonic at nearly the measured pressure and also the relative magnitude of the two harmonics agrees well. The Ti:Sapphire drive laser used for the HH source produces 30 fs (full width, half maximum) pulses with an energy of up to 8 mJ. We have investigated how the three free parameters (P, a, and L_m) affect the HH output for pulse energies E_p in the range from 0.5 to $6.0\,\mathrm{mJ}$. To visualise the regions that contribute to the phase-matched HH generation we plot in fig. 1 Δk as a function of radial position and time within the drive laser pulse for $E_p = 5\,\mathrm{mJ}$, $q = 27$, $a = 200\,\mu\mathrm{m}$ and $T_p = 30\,\mathrm{fs}$. The solid black line indicates where phase-matching is obtained and a small volume around this region contributes to the HH output.

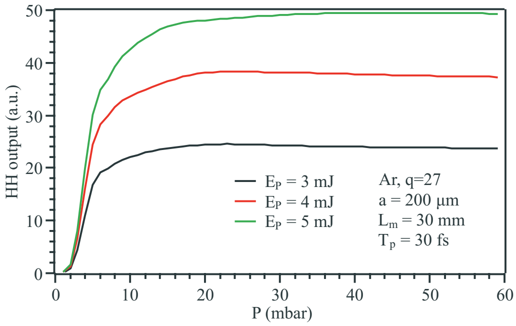

Figure 3: Scaling of the relative HH output at harmonic q=27 as a function of P for various drive laser pulse energies E_p.

The first parameter we varied was the radius a of the capillary. The capillary is filled with Argon gas at a pressure $P = 10\,\mathrm{mbar}$ and has a length $L_m = 30\,\mathrm{mm}$. Fig. 2 shows how the relative output at the $q = 27$ ($\lambda_q = 29.6\,\mathrm{nm}$) harmonic varies with the radius a for different pulse energies, while keeping the other parameters constant. Fig. 2 shows that the output at harmonic 27 increases by a factor of 500 when the pulse energy is increased from $0.5\,\mathrm{mJ}$ to $6\,\mathrm{mJ}$. However, this does not indicate that the efficiency increases by approximately a factor 50 as the optimum performance also depends on pressure and interaction length.

This is shown in figs. 3 and 4, where the dependency on pressure and length is plotted, respectively, for a radius $a = 200\,\mu\mathrm{m}$ and a few pulse energies near the optimum predicted by fig. 2. These figures indicate that the pressure used for the data in fig. 2 is below the optimum phase matching pressure, while the length of the capillary is near optimum. For $E_p = 5\,\mathrm{mJ}$ we calculate an optimum HH output of 50. To compare with measured data, we also modeled the configuration reported in ref. [4]. For a pulse energy $E_p = 0.25\,\mathrm{mJ}$, a pulse duration $T_p = 30\,\mathrm{fs}$, an interaction length $L_m = 30\,\mathrm{mm}$ we find a maximum output at harmonic 27 of 0.83 at a pressure $P = 28\,\mathrm{mbar}$. We thus find that the HH output is increased by a factor of 60, while

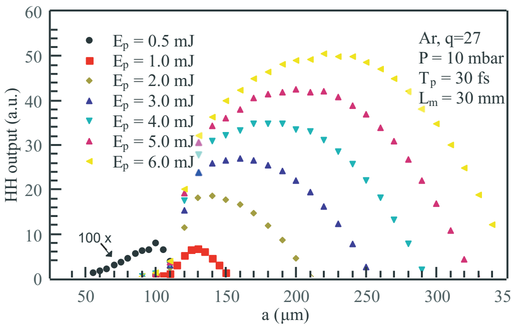

Figure 2: Scaling of the relative HH output at harmonic q=27 as a function of a for various drive laser pulse energies E_p.

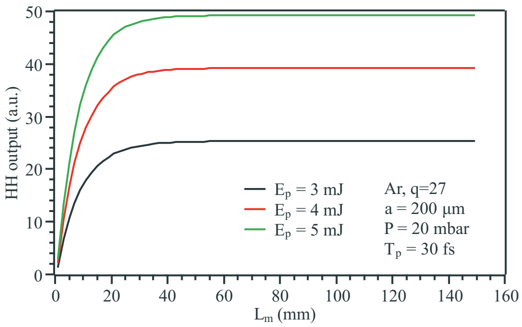

Figure 4: Scaling of the relative HH output at harmonic q=27 as a function of L_m for various drive laser pulse energies E_p.

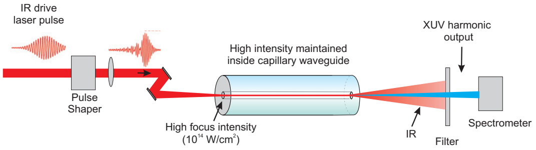

Figure 5: Schematic overview of the HHG setup.

the energy is only increased by a factor of 20. Thus, the conversion efficiency η_c improves by a factor of 3 for optimum HH generation at higher pulses energies. A further enhancement of up to a factor of 5 can be obtained with pulse shaping of the drive laser pulse [10].

Assuming optimal conditions for HH generation, the higher pulse energy combined with pulse shaping improves η_c from $10^{-6} - 10^{-5}$ [4] by a factor of 15 to $1.5 \times 10^{-5} - 1.5 \times 10^{-4}$. A conservative estimate for the energy coupled into the capillary is $6\,\mathrm{mJ}$ and we therefore expect about 90 to $900\,\mathrm{nJ}$ of energy for harmonic $q = 27\,(29.6\,\mathrm{nm})$. This corresponds to 4.5 to $45\,\mathrm{MW}$ peak power for a $20\,\mathrm{fs}$ duration of the harmonic.

HH SOURCE

The considerations given above show that in order to obtain HH pulses with a few to several tens of MW peak power, a drive laser pulse energy in the range of 5 to $6\,\mathrm{mJ}$ is required coupled into a capillary with a radius in the range 200 to $250\,\mu\mathrm{m}$. The drive laser pulse energy is delivered by a Coherent Mantis oscillator that seeds an Legend Elite amplifier system providing $8\,\mathrm{mJ}$ pulses with a $30\,\mathrm{fs}$ duration at a repetition rate of 1 kHz. For operation at FERMI@Elettra, the Mantis oscillator will be replaced by a Coherent Micra oscillator that is already installed at FERMI and synchronised to the FERMI master oscillator. This automatically locks the HH source to the timing system of FERMI. A schematic overview of the HH setup, as initially build at the University of Twente, is shown in fig. 5. For pulse shaping we implement a Dazzler in between the oscillator and amplifier. The control signal will be derived from the HH spectrum and an evolutionary algoritm provides the feedback to the Dazzler. A diagnostic station will be placed in between the Dazzler and amplifier to measure, a.o., the pulse shape. This diagnostic is used to protect the gratings in the amplifier chain from too high local energy density. Furthermore, this diagnostic is also a first indication of proper function of the control algoritm by comparing the pulse shape to known forms that provided the desired tuning and/or selective enhancement. It can be used as an online diagnostic tool. To measure the spectrum at the output of the HH source, various configurations are currently under evaluation.

DISCUSSION AND CONCLUSION

We have shown that by increasing the pulse energy used to drive the HH generation in a gas-filled capillary the conversion efficiency can be increased by a factor of 15 if pulse shaping is used. For Ar we show that at the 27^{th} harmonic $(29.6\,\mathrm{nm})$ peak powers of several tens of MW are possible. The same analysis will be repeated for Xe as HH medium to cover the longer wavelengths in the 30 to $60\,\mathrm{nm}$ range. The expected ouput is sufficient for seeding of FEL1 provided that the losses in the optical transport system are kept as small as possible. The required seed power is $\sim 1\,\mathrm{MW}$ at the undulator entrance. Therefore, the HH source will be placed near the undulator in the undulator hall to minimise the transport losses. The analysis has been done for the shortest wavelength of interest, as higher peak powers are expected at longer wavelengths. This will be verified using the method described in this paper. So far, HH generation from neutral atoms in a gas-filled capillary seems very promising as seed for HGHG, enabling seeded operation of FERMI@Elettra in the range of 10 to $6\,\mathrm{nm}$ using a single stage HGHG.

ACKNOWLEDGEMENT

This research is supported by the Dutch Technology Foundation STW, applied science division of NWO and the Technology Program of the Ministry of Economic Affairs, and by Coherent Europe B.V., The Netherlands.

REFERENCES

[1] A. L'Huillier et al., Phys. Rev. Lett **66** (1991) 2200.

[2] M. Schnürer et al., Phys. Rev. Lett. **80** (1998) 3236.

[3] Centre for X-ray Optics, `www-cxro.lbl.gov`.

[4] A. Rundquist et al., Science **280** (1998) 1412.

[5] C.G. Durfee et al., Phys. Rev. Lett. **83** (1999) 2187.

[6] P.B. Corkum, Phys. Rev. Lett. **71** (1993) 1994. M. Lewenstein et al., Phys. Rev A **49** (1994) 2117.

[7] C. Winterfeldt et al., Rev. Mod. Phys. **80** (2008) 117.

[8] C. Spielmann et al., IEEE J. Sel. Top. Quant. Electr. **4** (1998) 249.

[9] E. Constant et al., Phys. Rev. Lett. **82** (1999) 1668.

[10] T. Pfeifer et al., Appl. Phys. B **80** (2005) 277.